Fitting Spherical Objects in 3-D Point Cloud Using the Geometrical constraints

Van-Hung Le[1,2], Hai Vu [1], Thuy Thi Nguyen[3], Thi-Lan Le[1] and Thanh-Hai Tran[1]

Abstract

Estimating parameters of a primitive shape from a 3-D point cloud usually meets difficulties due to noises of data require a huge amount of computational time. The real point cloud of objects in the 3D environment have many noise and may be obscured when they are captured from Kinect version 1. In this paper, we utilize and analyse of spherical estimation steps from the point cloud data in Schnabel et al. [1]. From this, we propose a geometrical constraint to search 'good' samples for estimating spherical model and then apply to a new robust estimator named GCSAC (Geometrical Constraint SAmple Consensus). The proposed GCSAC algorithm takes into account geometrical constraints to construct qualified samples. Instead of randomly drawing minimal subset sample, we observe that explicit geometrical constraint of spherical model could drive sampling procedures. At each iteration of GCSAC, the minimal subset sample is selected by two criteria (1) They ensure consistency with the estimated model via a roughly inlier ratio evaluation; (2) The samples satisfy geometrical constraints of the interested objects. Based on the qualified samples, model estimation and verification procedures of a robust estimator are deployed in GCSAC. Comparing with the common robust estimators of RANSAC family (RANSAC, PROSAC, MLESAC, MSAC, LO-RANSAC and NAPSAC), GCSAC overperforms in term of both precisions of the estimated model and computational time. The implementations and evaluation datasets of the proposed method are made publicly available.

Index Terms

Robust Estimator; Primitive Shape Estimation; RANSAC and RANSAC Variations; Quality of Samples; Point Cloud data.

I. INTRODUCTION

ESTIMATING parameters of a primitive shape using robust estimators is a fundamental research in the fields of robotic and computer vision. To build the aiding system for visually impaired people or robot control system for object grasping then objects detection, pose estimation of object in the 3D environment are the important steps. Therein, the object detection that using the primitive shapes detection from the point cloud data of objects is a

[1]International Research Institute MICA, HUST - CNRS/UMI-2954 - GRENOBLE INP, Vietnam
[2] Tan Trao University, Vietnam lehung231187@gmail.com
[2]Faculty of Information Technology, VietNam National University Agriculture, Vietnam

method. Currently, many robust estimators have been proposed such as Hough Transform [2], RANSAC [3], RANSAC variations (e.g., MLESAC [4], PROSAC [5], LO-RANSAC [6], etc). RANSAC is a efficient iteration algorithm that is proposed by Fischler et al. [3] since 1981. Originally, a RANSAC paradigm draws randomly a Minimal Sample Set (MSS) from a point cloud data without any assumptions. As a result, RANSAC must run a relatively large number of iterations to find an optimal solution before stopping criterion. To improve performances, RANSAC-based methods [7] focus on either a better hypothesis from random samples or higher quality of the samples satisfying the estimated model. In this paper, we tackle a new sampling procedure which utilizes geometrical constraints to qualify a MSS. The MSS consisting of *good samples* is expected to generate better hypotheses, and as result, the better-estimated models are achievable. We examine the proposed method with fitting a sphere.

In the proposed robust estimator, a MSS is a stack consisting of samples which ensure two criteria: (1) The selected samples must ensure being consistent with the estimated model via a roughly inlier ratio evaluation; (2) The samples satisfy geometrical constraints of the interested objects (e.g., sphere constraints). The proposed constraints come from the explicit geometrical properties of the interested shapes. The good samples of the current stack are highly expected to generate a consensus set which quickly reaches to the maximal inlier ratio. Consequently, the number of iterations could be adaptively updated (as the termination manner of the adaptive RANSAC [8]). In GCSAC, we utilize the maximum log-likelihood of MLESAC algorithm to evaluate the estimated model. Finally, the effectiveness of the proposed method is confirmed by fitting results of a spherical object. The evaluations compare the performances of the proposed method and common RANSACs as original RANSAC, PROSAC, MLESAC, MSAC [4], LO-SAC, NAPSAC [9]. The implementations of the proposed method and evaluation datasets are made publicly available.

II. RELATED WORK

For a general introduction and performances of RANSAC family, readers can refer to good surveys in [10], [7]. In the context of this research, we briefly survey related works which are categorized into two topics. First, efficient schemes on the selection of minimal subset of samples for RANSAC-based robust estimators; and second, techniques for estimating a primitive shape, that focus into the fitting a spherical.

For the first topic, because the original RANSAC is very general with a straightforward implementation, it always requires considerable computational time. Many RANSAC variants have been proposed with further optimization for a minimal sample set (MSS) selection. Progressive Sample Consensus or PROSAC [5] orders quality of samples through a similarity function of two corresponding points in the context of finding good matching features between a pair of images. In PROSAC algorithm, the most promising hypotheses are attempted earlier, therefore drawing the samples is implemented in a more meaningful order. However, PROSAC faces critical issues for defining the similarity function. LO-RANSAC [6] and its fixed version LO$^+$-RANSAC [11] add local optimization steps within

RANSAC to improve accuracy. To speed up the computation, adaptive RANSAC [8] probes the data via the consensus sets in order to adaptively determine the number of selected samples. The algorithm is immediately terminated when a smaller number of iterations has been obtained. With the proposed method, the *good samples* are expected to generate the best model as fast as possible. Therefore, the termination condition of the adaptive RANSAC [8] should be explored. Recently, USAC [12] introduces a new frame-work for a robust estimator. In the USAC frame-work, some strategies such as the sample check (Stage 1b) or the model check (Stage 2b), before and after model estimation, respectively, are similar to our ideas in this work. However, USAC does not really deploy an estimator for primitive shape(s) from a point cloud. A recent work [13] proposes to use geometric verification within a RANSAC frame-work. The authors deployed several check procedures such as sample relative configuration check based on the epipolar geometry. Rather than the "check" procedures, our strategies anticipate achieving the best model as soon as possible. Therefore, the number of iterations is significantly reduced thanks to the results of the search for good sample process. The RANSAC-based algorithm used in the method of Chen et al. [14] and Aiger et al. [15] for registering of partially overlapping range images and partial surfaces of a 3D object.

For primitive shape estimation from 3-D point clouds, readers can refer to a survey on feature-based techniques [16]. Some fitting techniques, for instance, multiscale super-quadric fitting in [17], Hough transform in [18], are commonly used. Marco et al. [19], Anas et al. [20] used the 3D Hough Transform to estimate, extract sphere from point cloud data. However, the robust estimators (e.g., RANSAC family [7]) are always preferred techniques. Original RANSAC [3] demonstrates itself robust performances in estimating cylinders from range data. The authors in [21] and [1] formulate primitive shapes (e.g., line, plane, cylinder, sphere, cone) using two to seven parameters such as a cylinder has seven parameters, a sphere has four parameters, a cone has seven parameters, etc. Schnabel et al. [1] defines primitive shapes through some samples and their normal vectors. In this study, geometrical analysis of a sphere in [1] is adopted for defining criteria of the qualified samples as well as for estimating parameters of the interested model from a 3-D point cloud.

III. PROPOSED METHOD

A. Overview of the proposed robust estimator - GCSAC

To estimate parameters of a primitive shape, all of RANSAC variations in the RANSAC family [7] (RANSAC, MLESAC, PROSAC, MSAC, LOSAC, NAPSAC, .etc) implemented some steps as follows: drawing randomly a Minimal Sample Set (MSS)(RANSAC, MLESAC, MSAC) or semi-random (PROSAC) or using constraints of the sample's distribution (NAPSAC); estimating the model; evaluating the model and choosing the best model. This scheme is repeated K iterations. All of them are shown in the top panel of Fig. 1.

In this study, abilities of the proposed robust estimator (GCSAC) will be consolidated with a sphere. An overview of GCSAC algorithms is shown in the button panel of Fig. 1.

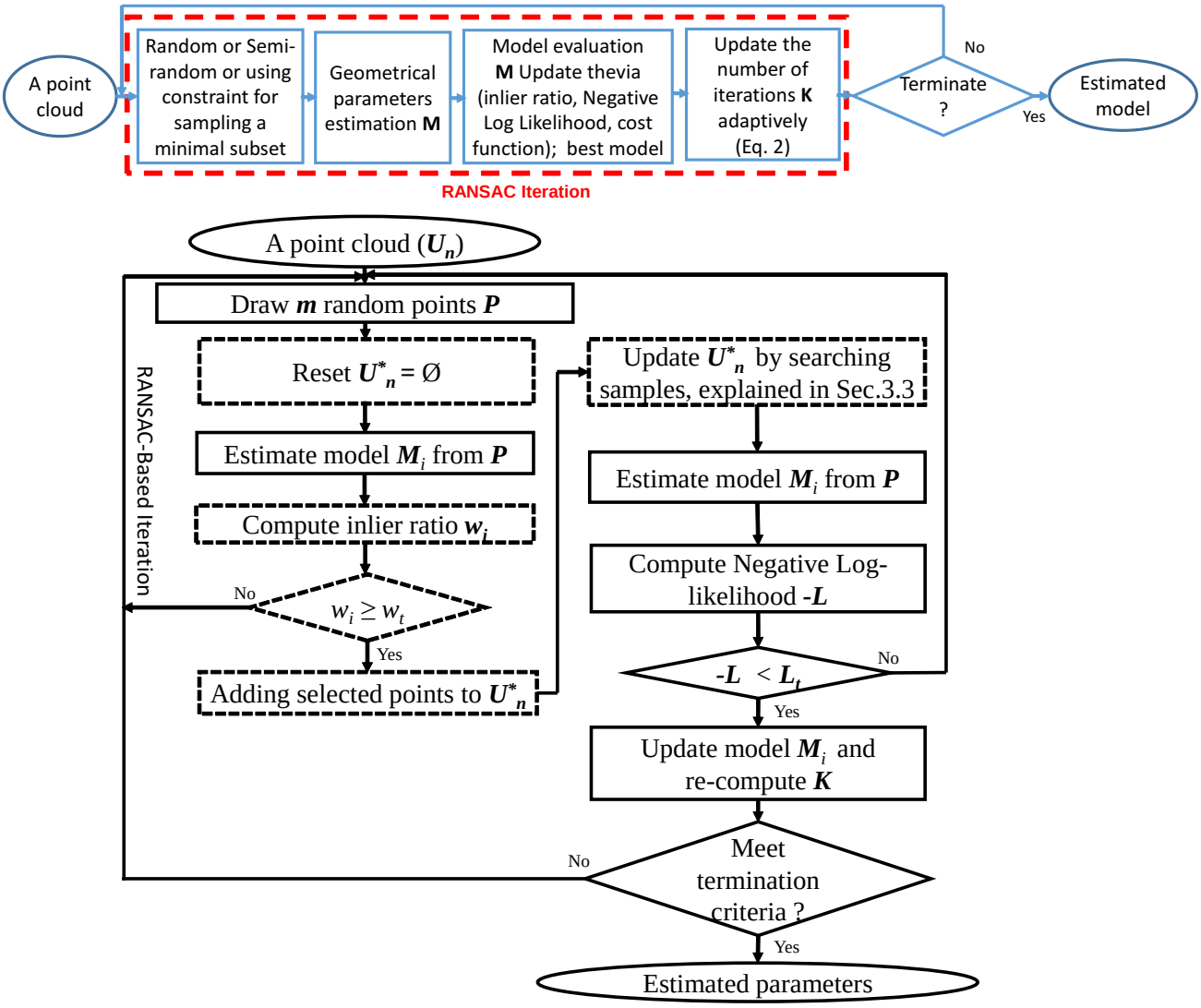

Fig. 1. Top panel: Over view of RANSAC-based algorithm. Bottom panel: A diagram of the GCSAC's implementations.

Following sections will explain the details of GCSAC's implementations.

The proposed GCSAC constructs a MSS by the random sampling and sampling using geometrical constraints of each primitive shape estimation, the aim of it is the generating the consensus of samples to be easy. To do this, a low inlier threshold is pre-determined. After only (few) random sampling iterations, the candidates of good samples could be achieved. Once initial MSS is established, its samples will be updated by the qualified one (or good sample) so that the geometrical constraints of the interested object is satisfied. The

estimated model is evaluated according to Maximum Log-likelihood criteria as MLESAC [4]. The final step is to determine the termination condition, which is adopted from the adaptive RANSAC algorithm [8]. Once the higher inlier ratio is obtained, the criterion termination K for determining the number of sample selection is updated by:

$$K = \frac{log(1-p)}{log(1-w^m)} \tag{1}$$

where p is the probability to find a model describing the data, m is the minimal number of samples to estimate a model, w is percentage of inliers in the point cloud. While p often to set a fixed value (e.g., $p = 0.99$ as a conservative probability), K therefore depends on w and m. The algorithm terminates as soon as the number of iterations of current estimation is less than that has already been performed.

Details of the GCSAC's implementation are given in Fig. 1. Obviously, the criteria which define the good samples are the most important. Based on the idea of adaptive RANSAC [8] to probe initial samples, GCSAC starts from roughly select of initial good samples. At each iteration, we assume that the worst case of inlier ratio $w_t = 0.1(10\%)$ is determined, to initialize the stack U_n^*, where U_n^* is used to store $m-1$ kept points and its inlier ratio w_i. A consensus set, therefore containing more than 10% of the data is easily found. A model is estimated from m random samples. As estimating a sphere is $m = 2$ [1]. After that, U_n^* is reset. m samples and the inlier ratio w_i of the estimated model is stored into U_n^* if w_i is equal to or greater than w_t. And then, the MSS utilizes $m-1$ kept *good* samples. The remaining m^{th} sample will be replaced by a better one which best satisfies the *geometrical constraints* of the interested shape. The good samples which satisfy the geometrical principles of a primitive shape are explained in Section III-B. If none of the iterations find out that satisfies $w_i \geq w_t$, the estimation algorithm degrades to the original MLESAC. The inlier ratio of the iteration depends on the threshold T, which chooses an optimal T value is out of the scope of this research.

B. Geometrical analyses and constraints for qualifying good samples

The geometrical model of a spherical object can be presented by four geometrical parameters [1]. In following sections, the principles of 3-D sphere are explained. Based on this geometrical analysis, the related constraints are given to select good samples.

1) Geometrical analysis for a spherical object: A sphere is determined by the following parameters: a centroid point which is denoted as $I_{sp}(x_0, y_0, z_0)$; its radius R_{sp}. To estimate sphere's parameters, Schnabel et al. [1] propose to use two points (p_1, p_2) with their corresponding normal vectors $(\mathbf{n}_1, \mathbf{n}_2)$ (see Fig. 2(a)). The centroid I_{sp} (a pink point Fig. 2(c)) is a middle point of the shortest line (a green line of Fig. 2(b)) which segments two lines given by $(p_1, \mathbf{n}_1)$ and $(p_2, \mathbf{n}_2)$. Identifying two lines $pa = p_1 + t * \mathbf{n}_1$ and $pb = p_2 + t * \mathbf{n}_2$ are shown in Fig. 2(b). t is the parameter of two lines pa, pb formulations. The radius R_{sp}

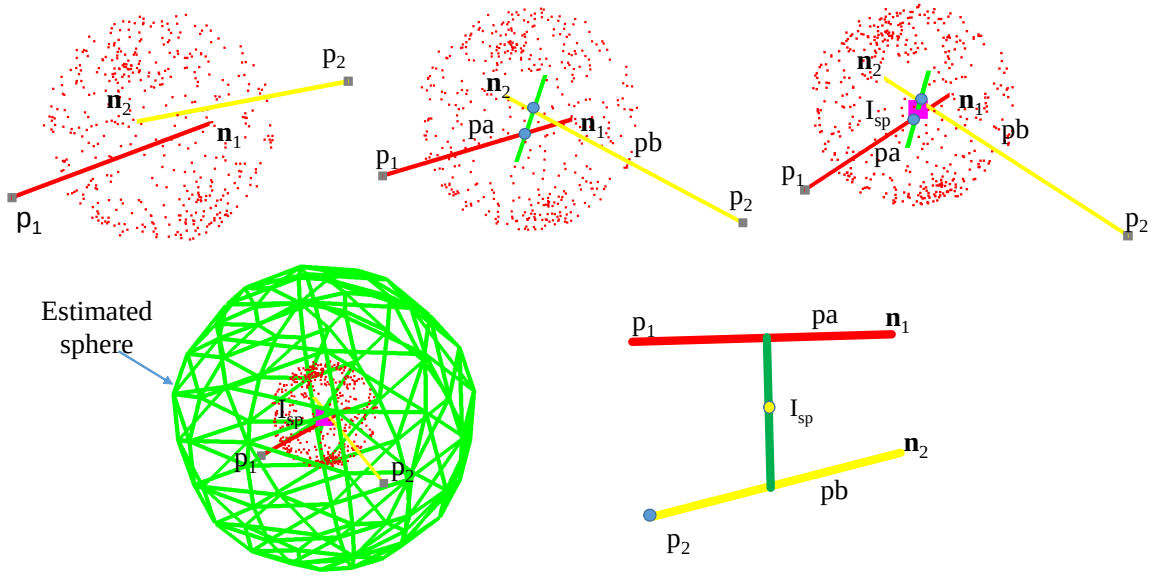

Fig. 2. Estimating parameters of a sphere from 3-D points. Red points are inlier points. In this figure, p_1, p_2 is two selected samples for estimating a sphere (two gray points), they are outlier points. Therefore, the estimated sphere is wrong of centroid and radius (see green sphere (d)). The sub-figures are illustrated in different view-points to clearly observe normal vectors for the geometrical analysis.

is determined by averaging the distance of I_{sp} to p_1 and I_{sp} to p_2. The estimated sphere is shown in Fig. 2(d).

The proposed geometrical constraints for fitting spherical objects: As above denoted, a sphere is estimated from two points (p_1, p_2) and their normal vectors $(\mathbf{n}_1, \mathbf{n}_2)$. In GCSAC, once stack U_n^* consisting of initial good samples is specified, we store p_1 and search p_2 in U_n and difference p_1 ($p_2 \in \{U_n \setminus p_1\}$). We observe that to generate a sphere, the triangle $(p_1 I_{sp} p_2)$ should be an isosceles, as shown in Fig. 2(e). This observation could be formulated by:

$$sh_p = \arg \min_{p_2 \in \{U_n \setminus p_1\}} \{(\| p_1 I_{sp} \| - \| p_2 I_{sp} \|)\} \tag{2}$$

The geometrical constraints in Eq. (2) means that if sh_p is close to 0 then the triangle $p_1 I_{sp} p_2$ is nearly isosceles one.

IV. EXPERIMENTAL RESULT

A. Dataset

The proposed method is warped by C++ programs using a PCL 1.7 library on a PC with Core i5 processor and 8G RAM. The program runs sequentially as a single thread. We have evaluated performances of GCSAC on synthesized datasets of the cylinder, sphere

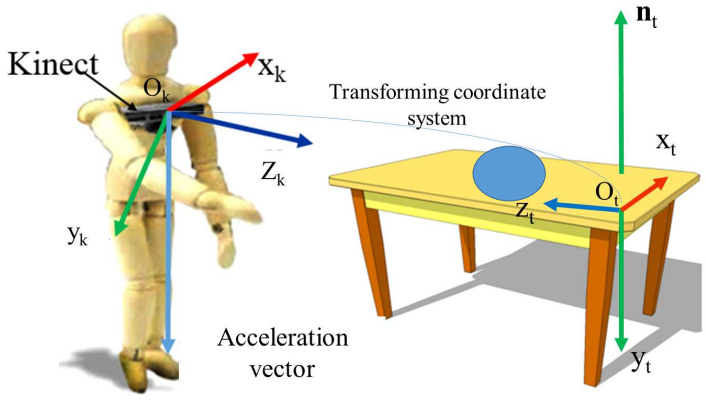

Fig. 3. Illustrating of our setup to collect the dataset

and cone. Each dataset consists of six different subsets. Characteristics of each subset are described in Table I. Major differences could be σ of the normal distribution for generating outlier/inlier data; or the spatial distribution of inliers.

For the sphere dataset *('first sphere')*, they are denoted from dC_1 to dC_6. In each subset dC_i, inlier ratio is increased by a step of 5% from 15 to 80 %. Therefore, there are fourteen point clouds. They are denoted dS_1 to dS_{14}. They have the maximal distance to true sphere 0.025 (or 2.5cm). Outliers are generated randomly in the limitation as Tab. I. A point cloud dS_i consists of 3000 points. These point clouds are generated from the curved surface of a true sphere: $x^2 + y^2 + z^2 = 1$. We also generate random points outside the surface of the sphere as outliers.

Moreover, we also evaluated on a real datasets. This is the dataset of two balls in four scenes, each scene has been included 500 frames and each frame has a ball on the table. It named *'second sphere'*. The setup of our experiment implemented a similar as [22] and is illustrated in Fig. 3.

To separate the data of a ball on the table, we have to implement some steps as below. First is the table plane detection that used the method in [23]. After that, the original coordinate is rotated and translated that the y-axis is parallel with the normal vector of the table plane as Fig. 3. The point cloud data of balls is separated with the point cloud data of the table plane. It is illustrated in Fig. 5.

B. Evaluation Measurements

Let notate a ground-truth of model $\mathbf{M}_t(x_t, y_t, z_t, r_t)$ and the estimated one $\mathbf{M}_e(x_e, y_e, z_e, r_e)$ where (x_t, y_t, z_t), (x_e, y_e, z_e) are the coordinates of the center points, r_t, r_e are the radius. To evaluate the performance of the proposed method, we use following measurements:

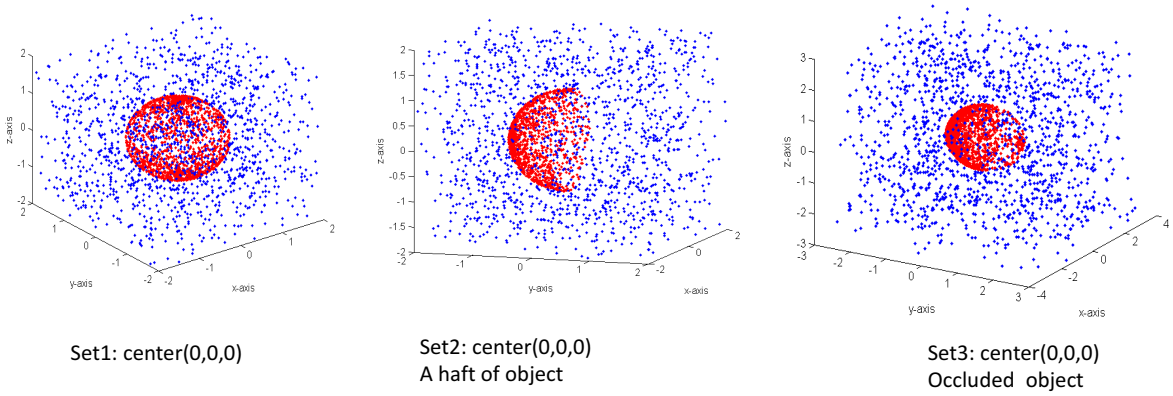

Fig. 4. Point clouds of dC_1, dC_2, dC_3 of the *'second sphere'* dataset (the synthesized data) in case of 50% inlier ratio. The red points are inliers, whereas blue points are outliers.

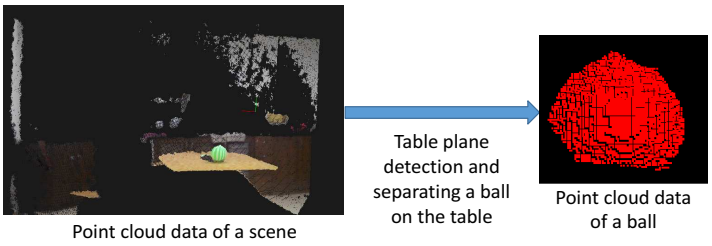

Fig. 5. Illustrating the separating the point cloud data of a ball in the scene.

- Let denote the relative error E_w of the estimated inlier ratio. The smaller E_w is, the better the algorithm is.

$$E_w = \frac{|w - w_{gt}|}{w_{gt}} \times 100 \tag{3}$$

where w_{gt} is the defined inlier ratio of ground-truth; w is the inlier ratio of the estimated model.

$$w = \frac{\#\text{inliers}}{\#\text{number of samples}} \tag{4}$$

- The total distance errors S_d [24] is calculated by summation of distances from any point p_j to the estimated model M_e. S_d is defined by:

$$S_d = \sum_{j=1}^{N} d(p_j, M_e) \tag{5}$$

TABLE I
THE CHARACTERISTICS OF THE GENERATED SPHERE DATASET (SYNTHESIZED DATASET)

Dataset	Characteristics of the generalized data		
	Radius	Spatial distribution of inliers	Spread of outliers
dC1, dC4	1	Around of a sphere	[-3, 3], [-4, 4]
dC2, dC5	1	Around of a sphere	[-3, 3], [-4, 4]
dC3, dC6	1	one half of a sphere	[-3, 3], [-4, 4]

- The processing time t_p is measured in milliseconds (ms). The smaller t_p is the faster the algorithm is.
- The relative error of the estimated center (only for synthesized datasets) E_d is Euclidean distance of the estimated center E_e and the truth one E_t. It is defined by:

$$E_d = |E_e - E_t| \tag{6}$$

- The relative error of the estimated radius E_r is different of the estimated radius r_e and the truth one r_t. It is defined by:

$$E_r = \frac{|r_e - r_t|}{r_t} \times 100\% \tag{7}$$

The proposed method (GCSAC) is compared with six common ones in RANSAC family. They are original RANSAC, PROSAC, MLESAC, MSAC, NAPSAC, LO-RANSAC. For setting the parameters, we fixed thresholds of the estimators with $T = 0.05$ (or 5cm), $w_t = 0.1$, $s_r = 3$ (cm). T is a distance threshold to set a data point to be inlier or outlier. s_r is the radius of a sphere when using NAPSAC algorithm. For the fair evaluations, T is set equally for all seven fitting methods.

C. The evaluation results

The performances of each method of the synthesized datasets are reported in Tab. II. For whole three datasets, GCSAC obtains the highest accuracy and lowest computational time. More generally, even using same criteria as MLESAC, the proposed GCSAC obtains better estimated model as shown by E_w measurements. The experimental results also confirmed the proposed constraints are working well with different primitive shapes. Although E_w of the sphere dataset is high ($E_w = 19.44\%$), this result is still better than the result of the compared methods. Among the compared RANSACs, it is interesting that original RANSAC generally give stable results for estimating a sphere. However, original RANSAC requires a high computational time. The proposed GSSAC estimates the models slightly better than the original RANSAC.

Table III also shown the fitting results of GCSAC method are more accurate than RANSAC variations. The results on the *'second sphere'* are high on all of the methods such

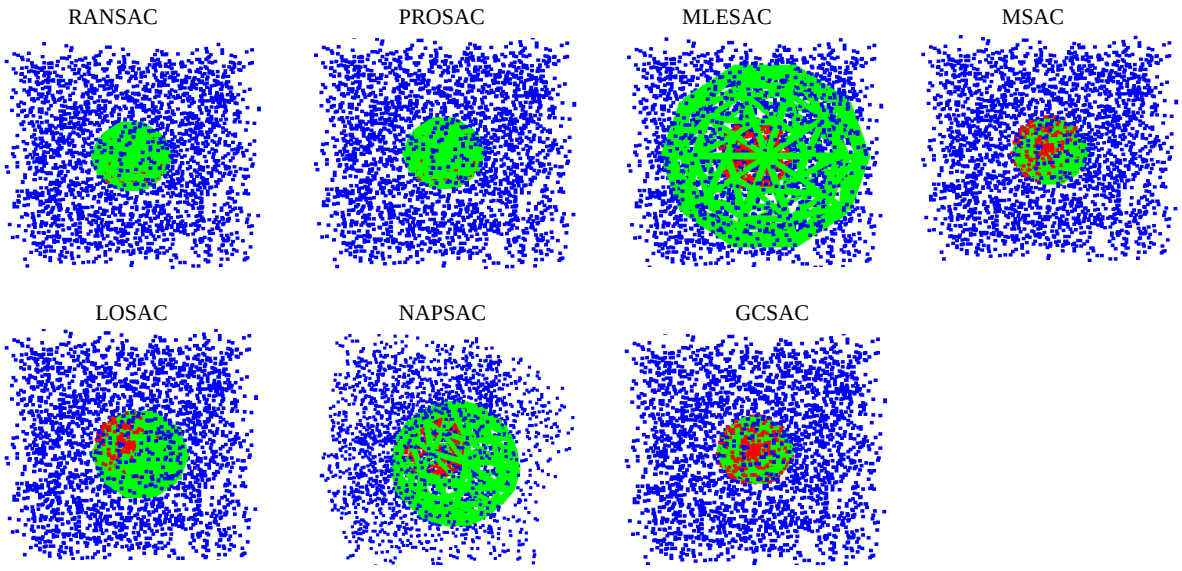

Fig. 6. Illustrating the fitting sphere of GCSAC and some RANSAC variations on the synthesized datasets, which have 15% inlier ratio. Red points are inlier points, blue points are outlier points. The estimated sphere is a green sphere.

TABLE II
THE AVERAGE EVALUATION RESULTS OF SYNTHESIZED DATASETS. THE SYNTHESIZED DATASETS WERE REPEATED 50 TIMES FOR STATISTICALLY REPRESENTATIVE RESULTS.

Dataset/ Method	Measure	**RANSAC**	**PROSAC**	**MLESAC**	**MSAC**	**LOSAC**	**NAPSAC**	**GCSAC**
'first sphere'	$E_w(\%)$	23.01	31.53	85.65	33.43	23.63	57.76	**19.44**
	S_d	3801.95	3803.62	3774.77	3804.27	3558.06	3904.22	**3452.88**
	$t_p(ms)$	10.68	23.45	1728.21	9.46	31.57	2.96	6.48
	$E_d(cm)$	0.05	0.07	1.71	0.08	0.21	0.97	0.05
	$E_r(\%)$	2.92	4.12	203.60	5.15	17.52	63.60	**2.61**

as the result of GCSAC when using the w measure is 100%, it is illustrated in Fig. 7(a). Due to the ball data has a small noise ratio and the threshold T to determine inlier points is large (0.05(5cm)). While the radius of a ball is 5cm to 7cm. All of the results shown, the performance of GCSAC is better than the RANSAC variations when implements estimating primitive shapes on the point cloud data, that has low inlier ratio (less than 50%). They were also shown, can use to the GCSAC algorithm for detecting, finding spherical objects in the real scenario. As a visually impaired person come to a sharing room or a kitchen to find a ball on the floor.

TABLE III
THE AVERAGE EVALUATION RESULTS ON THE *'second sphere'* DATASETS. THE REAL DATASETS WERE REPEATED 20 TIMES FOR STATISTICALLY REPRESENTATIVE RESULTS.

Dataset/ Method	Measure	**RANSAC**	**PROSAC**	**MLESAC**	**MSAC**	**LOSAC**	**NAPSAC**	**GCSAC**
'second sphere'	$w(\%)$	99.77	99.98	99.83	99.80	99.78	98.20	**100.00**
	S_d	29.60	26.62	29.38	29.37	28.77	35.55	**11.31**
	$t_p(ms)$	3.44	3.43	4.17	2.97	7.82	4.11	**2.93**
	$E_r(\%)$	30.56	26.55	30.36	30.38	31.05	33.72	**14.08**

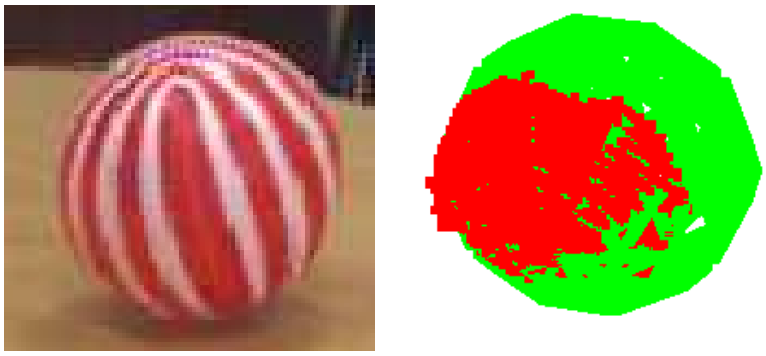

Fig. 7. Results of ball and cone fittings. The point cloud data of a ball is red points; the estimated spherical is marked as green points.

V. CONCLUSIONS

In this paper, we proposed GCSAC that is a new RANSAC-based robust estimator for fitting the primitive shapes from point clouds. The key idea of GCSAC is the combination of ensuring consistency with the estimated model via a roughly inlier ratio evaluation and geometrical constraints of the interested shapes that help to select good samples for estimating a model. Our proposed method is examined with common shapes (e.g., a sphere). The experimental results confirmed on the synthesized, real datasets that it works well even the point clouds with low inlier ratio. The results of the GCSAC algorithm compared to the RANSAC variations in the RANSAC family. In the future, we continue to validate GCSAC on other geometrical structures and evaluate the proposed method with the real scenario of detecting multiple objects.

ACKNOWLEDGMENT

This research is funded by Vietnam National Foundation for Science and Technology Development (NAFOSTED) under grant number 102.01-2017.315

REFERENCES

[1] R. Schnabel, R. Wahl, and R. Klein. Efficient ransac for point-cloud shape detection. *Computer Graphics Forum*, 26(2):214–226, 2007.

[2] B. Dorit, J.E. Kai Lingemann, and N. Andreas. Real-Time Table Plane Detection Using Accelerometer Information And Organized Point Cloud Data From Kinect Sensor. *Journal of Computer Science and Cybernetics*, pages pp, 243–258, 2016.

[3] M. A. Fischler and R.C. Bolles. Random sample consensus: A paradigm for model fitting with applications to image analysisand automated cartography. *Communications of the ACM*, 24(6):pp, 381–395, 1981.

[4] Philip H. S. Torr and A. Zisserman. Mlesac: A new robust estimator with application to estimating image geometry. *Computer Vision and Image Understanding*, 78(1):pp, 138–156, 2000.

[5] O. Chum and J. Matas. Matching with prosac progressive sample consensus. In *Procedings of the IEEE Computer Society Conference on Computer Vision and Pattern Recognition (CVPR'05)*, pages pp, 220–226, 2005.

[6] O. Chum, J. Matas, and J. Kittler. Locally optimized ransac. In *DAGM-Symposium*, volume 2781 of *Lecture Notes in Computer Science*, pages pp, 236–243. Springer, 2003.

[7] S. Choi, T. Kim, and W. Yu. Performance evaluation of ransac family. In *Procedings of the British Machine Vision Conference 2009*, pages pp, 1–12. British Machine Vision Association, 2009.

[8] R.I. Hartley and A. Zisserman. *Multiple View Geometry in Computer Vision*. Cambridge University Press, ISBN: 0521540518, second edition, 2004.

[9] D.R. Myatt, P.H.S. Torr, S.J. Nasuto, J.M Bishop, and R. Craddock. Napsac: high noise, high dimensional robust estimation. In *Procedings of the British Machine Vision Conference (BMVC'02)*, pages pp, 458–467, 2002.

[10] R. Raguram, JM. Frahm, and M. Pollefeys. A comparative analysis of ransac techniques leading to adaptive real-time random sample consensus. In *Procedings of the European Conference on Computer Vision. (ECCV'08)*, pages pp, 500–513, 2008.

[11] K. Lebeda, J. Matas, and O. Chum. Fixing the locally optimized ransac. In *Proceedings of the British Machine Vision Conference 2012.*, pages pp, 3–7, 2012.

[12] R. Raguram, O. Chum, M. Pollefeys, J. Matas, and J. M. Frahm. Usac: A universal framework for random sample consensus. *IEEE Transactions on Pattern Analysis and Machine Intelligence*, 35(8):pp, 2022–2038, Aug 2013.

[13] M. Kohei, U. Yusuke, S. Shigeyuki, and S. Shinichi. Geometric verification using semi-2d constraints for 3d object retrieval. In *Proceedings of the International Conference on Pattern Recognition (ICPR) 2012.*, pages pp, 2339–2344, 2016.

[14] C.S. Chen, Y.P. Hung, and J.B. Cheng. RANSAC-based DARCES: a new approach to fast automatic registration of partially overlapping range images. *IEEE Transactions on Pattern Analysis and Machine Intelligence*, 21(11):pp, 1229 –1234, 1999.

[15] Aiger D., N. J. Mitra, and D. Cohen-Or. 4-points congruent sets for robust surface registration. *ACM Transactions on Graphics*, 27(3), 2008.

[16] K. Alhamzi and M Elmogy. 3d object recognition based on image features : A survey. *International Journal of Computer and Information Technology (ISSN: 2279 0764)*, 03(03):pp, 651–660, 2014.

[17] K. Duncan, S. Sarkar, R. Alqasemi, and R. Dubey. Multiscale superquadric fitting for efficient shape and pose recovery of unknown objects. In *Procedings of the International Conference on Robotics and Automation (ICRA'2013)*, 2013.

[18] G. Osselman, B. Gorte, G. Sithole, and T. Rabbani. Recognising structure in laser scanner point clouds. In *International Archives of Photogrammetry, Remote Sensing and Spatial Information Sciences*, pages pp, 33–38, 2004.

[19] C. Marco, V. Roberto, and C. Rita. 3d hough transform for sphere recognition on point clouds. *Machine Vision and Applications*, pages pp, 1877–1891, 2014.

[20] A. Anas, N. Mark, and C. John. Sphere detection in kinect point clouds via the 3d hough transform. In *International Conference on Computer Analysis of Images and Patterns*, 2013.

[21] S. Garcia. Fitting primitive shapes to point clouds for robotic grasping. *Master Thesis in Computer Science (30 ECTS credits) at the School of Electrical Engineering Royal Institute of Technology*, 2009.

[22] Le V.H., Vu H., , Nguyen T.T., Le T.L., Tran T.H., Da T.C., and Nguyen H.Q. Geometry-based 3-d object fitting and localization in grasping aid for visually impaired. In *The Sixth International Conference on Communications and Electronics*. IEEE-ICCE, 2016.

[23] Le V.H., M. Vlaminck, Vu H., , Nguyen T.T., Le T.L., Tran T.H., Luong Q.H., P. Veelaert, and P. Wilfried. Real-Time Table Plane Detection Using Accelerometer Information And Organized Point Cloud Data From Kinect Sensor. *Journal of Computer Science and Cybernetics*, pages pp, 243–258, 2016.

[24] P. Faber and R.B. Fisher. A Buyer's Guide to Euclidean Elliptical Cylindrical and Conical Surface Fitting. In *Procedings of the British Machine Vision Conference 2001*, number 1, pages pp, 54.1–54.10, 2001.